

Stochastic Optimally-Tuned Ranged-Separated Hybrid Density Functional Theory

Daniel Neuhauser*

Department of Chemistry and Biochemistry, University of California at Los Angeles, CA-90095 USA

Eran Rabani†

Department of Chemistry, University of California and Materials Science Division,

Lawrence Berkeley National Laboratory, Berkeley, California 94720, USA and

The Sackler Center for Computational Molecular and Materials Science, Tel Aviv University, Tel Aviv, Israel 69978

Yael Cytter and Roi Baer‡

Fritz Haber Center for Molecular Dynamics, Institute of Chemistry,

The Hebrew University of Jerusalem, Jerusalem 91904, Israel

We develop a stochastic formulation of the optimally-tuned range-separated hybrid density functional theory which enables significant reduction of the computational effort and scaling of the non-local exchange operator at the price of introducing a controllable statistical error. Our method is based on stochastic representations of the Coulomb convolution integral and of the generalized Kohn-Sham density matrix. The computational cost of the approach is similar to that of usual Kohn-Sham density functional theory, yet it provides much more accurate description of the quasiparticle energies for the frontier orbitals. This is illustrated for a series of silicon nanocrystals up to sizes exceeding 3000 electrons. Comparison with the stochastic GW many-body perturbation technique indicates excellent agreement for the fundamental band gap energies, good agreement for the band-edge quasiparticle excitations, and very low statistical errors in the total energy for large systems. The present approach has a major advantage over one-shot GW by providing a self-consistent Hamiltonian which is central for additional post-processing, for example in the stochastic Bethe-Salpeter approach.

I. INTRODUCTION

First-principles descriptions of quasiparticle excitations in extended and large confined molecular systems are prerequisite for understanding, developing and controlling molecular electronic, optoelectronic and light-harvesting devices. In search of reliable theoretical frameworks, it is tempting to use Kohn-Sham density functional theory (DFT),¹ which provides accurate predictions of the structure and properties of molecular, nanocrystal and solid state systems. However, Kohn-Sham DFT (KS-DFT) approximations predict poorly quasiparticle excitation energies both in confined and in extended systems,²⁻⁴ even for the frontier occupied orbital energy, for which KS-DFT is expected to be exact.⁵⁻⁷ This has led to the development of two main first-principles alternative frameworks for quasiparticle excitations: many-body perturbation theory, mainly within the so-called GW approximation⁸ on top of DFT,⁹⁻²⁵ and generalized-KS DFT.²⁶⁻³⁰

Recently, range-separated hybrid (RSH) functionals³¹⁻³⁷ combined with an optimally-tuned range parameter^{38,39} were shown to very successfully predict quasiparticle band gaps, band edge energies and excitation energies for a range of interesting *small* molecular systems, well matching both experimental results and GW predictions.⁴⁰⁻⁴³ The key element of the range parameter tuning is the minimization of the deviation between the highest occupied orbital energy and the ionization energy^{39,40} or the direct minimization of the energy curvature.⁴⁴

The use of GW and the optimally-tuned RSH (OT-RSH) approaches for describing quasiparticle excitations in *extended* systems is hampered by high computational scal-

ing. The computational bottleneck in GW is in the calculation of the screened potential within the Random Phase Approximation (RPA) while in OT-RSH it is the application of non-local exchange to each of the molecular orbitals. OT-RSH is a self-consistent method and should therefore be compared to self-consistent GW calculations; however, the latter are extremely expensive as the self-energy operator must be applied to all Dyson orbitals.

Recently, we proposed a stochastic formulation limited to the G_0W_0 approach, where the computational complexity was reduced by combining stochastic decomposition techniques and real-time propagation to obtain the expectation value of the self-energy within the GW approximation.⁴⁵ The stochastic GW (sGW) was used to describe charge excitations in very large silicon nanocrystals (NCs) with $N_e > 3000$ (N_e is the number of electrons), with computational complexity scaling nearly linearly with the system size. Similar stochastic techniques have been developed by us for DFT,⁴⁶ for embedded DFT,⁴⁷ and for other electronic structure problems.⁴⁸⁻⁵²

Here we develop a stochastic formalism suitable for applying the OT-RSH functionals for studying quasiparticle excitations in *extended* systems. The approach builds on our previous experience with the exchange operator,⁵³⁻⁵⁵ but several new necessary concepts are developed here for the first time. We start with a brief review of the OT-RSH approach, then move on to describe the specific elements of the stochastic approach, and finally present results.

We dedicate this paper to Prof. Ronnie Kosloff from the Hebrew University to acknowledge his important contributions to the field of computational/theoretical chemistry. Kosloff has been our teacher and mentor for many years

and his methods, such as the Chebyshev expansions and Fourier grids,^{56,57} are used extensively in our present work as well.

II. OPTIMALLY-TUNED RANGE SEPARATED HYBRID FUNCTIONALS

For a systems of N_e electrons in an external one-electron potential $v_{ext}(\mathbf{r})$ having a total spin magnetization s_z in the z direction, the OT-RSH energy is a functional of the spin-dependent density matrix (DM) $\rho_{\uparrow,\downarrow}(\mathbf{r}, \mathbf{r}')$ given in atomic units as:

$$E_{RSH}^\gamma[\rho_\uparrow, \rho_\downarrow] = \text{tr} \left[\rho \left(-\frac{1}{2} \hat{\nabla}^2 + v_{ext}(\hat{\mathbf{r}}) \right) \right] + E_H[n] + E_{XC}^\gamma[n] + K_X^\gamma[\rho_\uparrow, \rho_\downarrow], \quad (1)$$

where γ is the range-parameter, discussed below, while

$$E_H[n] = \frac{1}{2} \iint u_C(|\mathbf{r} - \mathbf{r}'|) n(\mathbf{r}) n(\mathbf{r}') d\mathbf{r} d\mathbf{r}' \quad (2)$$

is the Hartree energy functional of the density $n(\mathbf{r}) = \rho(\mathbf{r}, \mathbf{r}) = \sum_{\sigma=\uparrow,\downarrow} \rho_\sigma(\mathbf{r}, \mathbf{r})$ and $u_C(r) = r^{-1}$ is the Coulomb potential energy. $E_{XC}^\gamma[n]$ is the unknown γ -dependent exchange-correlation energy functional which in practical applications is approximated. The non-local exchange energy functional is given by

$$K_X^\gamma[\rho_\uparrow, \rho_\downarrow] = -\frac{1}{2} \sum_{\sigma=\uparrow,\downarrow} \iint u_C^\gamma(|\mathbf{r} - \mathbf{r}'|) |\rho_\sigma(\mathbf{r}, \mathbf{r}')|^2 d\mathbf{r} d\mathbf{r}', \quad (3)$$

where $u_C^\gamma(r) = r^{-1} \text{erf}(\gamma r)$. This choice of $u_C^\gamma(r)$ accounts for long-range contributions to the non-local exchange energy and thus dictates a complementary cutoff in the *local* exchange-correlation energy, $E_{XC}^\gamma[n]$, to avoid overcounting the exchange energy.^{32,39,58}

When the exact $E_{XC}^\gamma[n]$ functional is used, minimizing $E_{RSH}^\gamma[\rho_\uparrow, \rho_\downarrow]$ with respect to $\rho_\sigma(\mathbf{r}, \mathbf{r}')$ under the constraints specified below leads to the exact ground-state energy and electron density $n(\mathbf{r})$. For approximate $E_{XC}^\gamma[n]$ approximate estimates of these quantities are obtained. To express the constraints we first require the spin-dependent DM to be Hermitian and thus expressible as:

$$\rho_\sigma(\mathbf{r}, \mathbf{r}') = \sum_j f_{j,\sigma} \phi_{j,\sigma}(\mathbf{r}) \phi_{j,\sigma}^*(\mathbf{r}'). \quad (4)$$

where $f_{j,\sigma}$ and $\phi_{j,\sigma}(\mathbf{r})$ are its eigenvalues and orthonormal eigenfunctions. The constraints are then given in terms of the eigenvalues $f_{j,\sigma}$ as:

$$0 \leq f_{j,\sigma} \leq 1, \quad (5)$$

$$\sum_{j,\sigma} f_{j,\sigma} = N_e, \quad (6)$$

$$\frac{1}{2} \sum_j (f_{j,\uparrow} - f_{j,\downarrow}) = s_z. \quad (7)$$

The necessary conditions for a minimum of $E_{RSH}^\gamma[\rho_\uparrow, \rho_\downarrow]$ is that $\phi_{j,\sigma}(\mathbf{r})$ obey the generalized KS equations:

$$\hat{h}_\sigma^\gamma \phi_{j,\sigma}^\gamma(\mathbf{r}) = \varepsilon_{j,\sigma}^\gamma \phi_{j,\sigma}^\gamma(\mathbf{r}), \quad (8)$$

where $\varepsilon_{j,\sigma}^\gamma$ are the spin-dependent eigenvalues of the generalized KS Hamiltonian ($j = 1, 2, \dots$ and $\sigma = \uparrow, \downarrow$) given by:

$$\hat{h}_\sigma^\gamma = -\frac{1}{2} \hat{\nabla}^2 + v_\sigma^\gamma(\hat{\mathbf{r}}) + \hat{k}_\sigma^\gamma. \quad (9)$$

Note that the DM and its eigenstates minimizing the energy functional $E_{RSH}^\gamma[\rho_\uparrow, \rho_\downarrow]$ are themselves γ -dependent and are thus denoted by $\rho_\sigma^\gamma(\mathbf{r}, \mathbf{r}')$, $\phi_{j,\sigma}^\gamma(\mathbf{r})$; the DM eigenvalues are not γ -dependent, as shown below. The one-electron Hamiltonian \hat{h}_σ^γ contains the kinetic energy, a local potential in r -space $v_\sigma^\gamma(\hat{\mathbf{r}})$ and a non-local exchange operator \hat{k}_σ^γ . The local r -space potential is further decomposed into three contributions:

$$v_\sigma^\gamma(\mathbf{r}) = v_{ext}(\mathbf{r}) + v_H(\mathbf{r}) + v_{XC,\sigma}^\gamma(\mathbf{r}), \quad (10)$$

where $v_H(\mathbf{r}) = \frac{\delta E_H[n]}{\delta n(\mathbf{r})} = \int n(\mathbf{r}') u_C(|\mathbf{r} - \mathbf{r}'|) d\mathbf{r}'$ is the Hartree potential and $v_{XC,\sigma}^\gamma(\mathbf{r}) = \frac{\delta E_{XC}^\gamma[n]}{\delta \rho_\sigma(\mathbf{r}, \mathbf{r})}$ is the short-range exchange-correlation potential. The non-local exchange operator $\hat{k}_\sigma^\gamma = \frac{\delta K_X^\gamma}{\delta \rho_\sigma} \Big|_{[\rho_\uparrow^\gamma, \rho_\downarrow^\gamma]}$ is expressed by its operation on a wave function $\psi_\sigma(\mathbf{r})$ of the same spin as:

$$\hat{k}_\sigma^\gamma \psi_\sigma(\mathbf{r}) = - \int u_C^\gamma(|\mathbf{r} - \mathbf{r}'|) \rho_\sigma^\gamma(\mathbf{r}, \mathbf{r}') \psi_\sigma(\mathbf{r}') d\mathbf{r}'. \quad (11)$$

In this work we consider closed shell systems where $s_z = 0$ and $N_e = 2N_H$ where N_H is the number of electron pairs, i.e., the level number of the highest occupied orbital. In this case, as in Hartree-Fock theory and DFT, the DM eigenvalues $f_{j,\sigma}$ which minimize $E_{RSH}^\gamma[\rho_\uparrow, \rho_\downarrow]$ are $f_{j,\sigma} = 1$ if $j \leq N_H$ and 0 otherwise.⁵⁹ Hence, these conditions are used *a-priori* as constraints during the minimization of $E_{RSH}^\gamma[\rho_\uparrow, \rho_\downarrow]$. However, for the tuning process the ensemble partial ionization of an up-spin (or down-spin) electron needs to be considered. Thus, these values for $f_{j,\sigma}$ are still used except for $j = N_H$ and $\sigma = \uparrow$ where $f_{H,\uparrow}$ is fixed to be a positive fraction (i.e., the negative of the overall charge of the system, $-c$) during the minimization of the GKS ensemble energy $E_{RSH}^\gamma[\rho_\uparrow, \rho_\downarrow]$ (for clarity, we abbreviate $N_H \equiv H$ for the frontier orbital energy (ε) and occupation (f)). We note in passing that tuning is often done by combining a linearity condition from the $N + 1$ electron system.⁶⁰ We leave this for future work, and state that it can be done along the same lines as described here for the N electron system.

The optimally-tuned range-parameter γ is determined from the requirement that the highest occupied generalized KS orbital energy $\varepsilon_{H,\sigma}^\gamma$ is independent of its occupancy

$f_{H,\sigma}$:

$$\frac{\partial \varepsilon_{H,\uparrow}^\gamma}{\partial f_{H,\uparrow}} = 0. \quad (12)$$

Through Janak's theorem⁶¹ this equation implies that the energy curvature $\frac{\partial^2 E_{RHS}^\gamma}{\partial f_{H,\uparrow}^2}$ is zero. In practical terms, Eq. (12) is solved by a graphical root search as shown in Fig. 1 and discussed below.

III. STOCHASTIC FORMULATION OF THE NON-LOCAL EXCHANGE OPERATOR

In real-space or plane-waves implementations the application of the Hamiltonian \hat{h}_{KS} on a single particle wave function involves a pair of Fast Fourier Transforms (FFT) to switch the wave function between k -space where the kinetic energy is applied and r -space for applying the potential energy.⁶³ Therefore, for a grid of N_g grid-points the operational cost is $10N_g \log_2 N_g$. The KS Hamiltonian operation scales quasi linearly with system size. The scaling is much steeper for the RSH Hamiltonian because the non-local exchange operator \hat{k}_σ^γ applies N_e Coulomb convolution integrals, each of which is done using an FFT of its own thus involving $10N_g \log_2 N_g \times N_e$ operations. Therefore, the GKS Hamiltonian operation which scales quasi-quadratically is much more time consuming than the KS Hamiltonian. Our approach, described next, reduces significantly the operation cost and even lowers the scaling due to the reduction of γ_* as the system size grows.

We first express the occupations in the DM in Eq. (4) as a combination of a occupations of a closed-shell density matrix and a remnant due to the overall charge of the molecule, c (assuming $-1 \leq c \leq 1$); This separation reduces the stochastic error later when the charge of the system is continuously varied, as needed for the optimal tuning. Thus:

$$\begin{aligned} \rho_\sigma(\mathbf{r}, \mathbf{r}') &= \sum_j f_{j,\sigma} \phi_{j,\sigma}(\mathbf{r}) \phi_{j,\sigma}^*(\mathbf{r}') \\ &= \sum_{j \leq N_H} \phi_{j,\sigma}(\mathbf{r}) \phi_{j,\sigma}^*(\mathbf{r}') - c \phi_{F\uparrow}(\mathbf{r}) \phi_{F\uparrow}^*(\mathbf{r}') \end{aligned} \quad (13)$$

where $\phi_{F\uparrow}$ is the frontier orbital being charged and c is the amount of charge. When tuning the neutral system $F = H$ is the HOMO and it is being positively charged (electrons removed from HOMO) so $c < 0$. When tuning for the anion $F = H + 1$ is the LUMO and the system being negatively charged (electrons are added to the LUMO) so $c > 0$. We assume without loss of generality that the spin of the charge frontier orbital is up. Next we evaluate the first term on the RHS of Eq. (14) using stochastic orbitals:

$$\sum_{j \leq N_H} \phi_{j,\sigma}(\mathbf{r}) \phi_{j,\sigma}^*(\mathbf{r}') = \langle \eta_\sigma(\mathbf{r}) \eta_\sigma^*(\mathbf{r}') \rangle_\xi, \quad (15)$$

where $\eta_\sigma(\mathbf{r})$ is a projected-stochastic orbital described in terms of the eigenstates of \hat{h}_σ (which can be alternatively obtained using a Chebyshev expansion of the relevant projection operator⁴⁶):

$$\eta_\sigma(\mathbf{r}) = \sum_{j \leq N_H} \phi_{j,\sigma}(\mathbf{r}) \langle \phi_{j,\sigma} | \xi \rangle, \quad (16)$$

and

$$\xi(\mathbf{r}) = \pm \frac{1}{\sqrt{h^3}} \quad (17)$$

is a stochastic orbital with a random sign (± 1) at each grid-point. (Note that application of Eq. (16) is itself a quadratic step however it is a "cheap" step as it is done only once in each SCF iteration.) With this, Eq. (11) is rewritten as:

$$\begin{aligned} \hat{k}_\sigma^\gamma \psi_\sigma(\mathbf{r}) &= - \left\langle \eta_\sigma(\mathbf{r}) \int u_C^\gamma(|\mathbf{r} - \mathbf{r}'|) \eta_\sigma^*(\mathbf{r}') \psi_\sigma(\mathbf{r}') d\mathbf{r}' \right\rangle_\xi \\ &+ c \int u_C^\gamma(|\mathbf{r} - \mathbf{r}'|) \phi_{F,\sigma}(\mathbf{r}) \phi_{F,\sigma}^*(\mathbf{r}') \psi_\sigma(\mathbf{r}') d\mathbf{r}' \end{aligned} \quad (18)$$

Next, we address the convolution in the random part of the above expression, by rewriting the range-separated Coulomb potential as

$$u_C^\gamma(|\mathbf{r} - \mathbf{r}'|) = \langle \zeta(\mathbf{r}) \zeta^*(\mathbf{r}') \rangle, \quad (19)$$

where $\zeta(\mathbf{r}) = (2\pi)^{-3} \int d\mathbf{k} \sqrt{\tilde{u}_C^\gamma(\mathbf{k})} e^{i\varphi(\mathbf{k})} e^{i\mathbf{k}\cdot\mathbf{r}}$, $\tilde{u}_C^\gamma(\mathbf{k})$ is the Fourier transform of $u_C^\gamma(\mathbf{r})$, and $\varphi(\mathbf{k})$ is a random phase between 0 and 2π at each k -space grid point. This can be seen by inserting the definition of $\zeta(\mathbf{r})$ into Eq. (19) and using the identity $\left\langle e^{-i[\varphi(\mathbf{k}) - \varphi(\mathbf{k}')] } \right\rangle_\varphi = (2\pi)^3 \delta(\mathbf{k} - \mathbf{k}')$. (See Appendix A for the treatment of the $k = 0$ term). The non-local exchange operation is finally written as:

$$\begin{aligned} \hat{k}_\sigma^\gamma \psi_\sigma(\mathbf{r}) &= - \left\langle \eta_\sigma(\mathbf{r}) \zeta(\mathbf{r}) \int \zeta^*(\mathbf{r}') \eta_\sigma^*(\mathbf{r}') \psi_\sigma(\mathbf{r}') d\mathbf{r}' \right\rangle_{\xi,\varphi} \\ &+ c \int u_C^\gamma(|\mathbf{r} - \mathbf{r}'|) \phi_{A,\sigma}(\mathbf{r}) \phi_{A,\sigma}^*(\mathbf{r}') \psi_\sigma(\mathbf{r}') d\mathbf{r}'. \end{aligned} \quad (20)$$

In actual applications we use a finite number N_χ of pairs of stochastic orbitals $\chi_\sigma(\mathbf{r}) = \zeta(\mathbf{r}) \eta_\sigma(\mathbf{r})$ and thus:

$$\begin{aligned} \hat{k}_\sigma^\gamma \psi_\sigma(\mathbf{r}) &= - \frac{1}{N_\chi} \sum_\chi \chi_\sigma(\mathbf{r}) \langle \chi_\sigma | \psi_\sigma \rangle \\ &+ c \delta_{\sigma,\uparrow} \int u_C^\gamma(|\mathbf{r} - \mathbf{r}'|) \phi_{A,\sigma}(\mathbf{r}) \phi_{A,\sigma}^*(\mathbf{r}') \psi_\sigma(\mathbf{r}') d\mathbf{r}'. \end{aligned} \quad (21)$$

The $\zeta(\mathbf{r})$'s are calculated once and stored in memory while the $\eta_\sigma(\mathbf{r})$'s are generated on the fly. The computational scaling of the non-local exchange operation on $\psi_\sigma(\mathbf{r})$ is thus $N_\chi N_g$ (vs. $10N_g \log_2 N_g \times N_e$ for the deterministic case). Typically, $N_\chi = 200$ and $N_g = 10^6$ and thus, the operation of the stochastic non-local exchange becomes comparable in terms of computational effort to that of operating with the kinetic energy, so the computational cost of applying the GKS Hamiltonian is similar to that of the KS Hamiltonian.

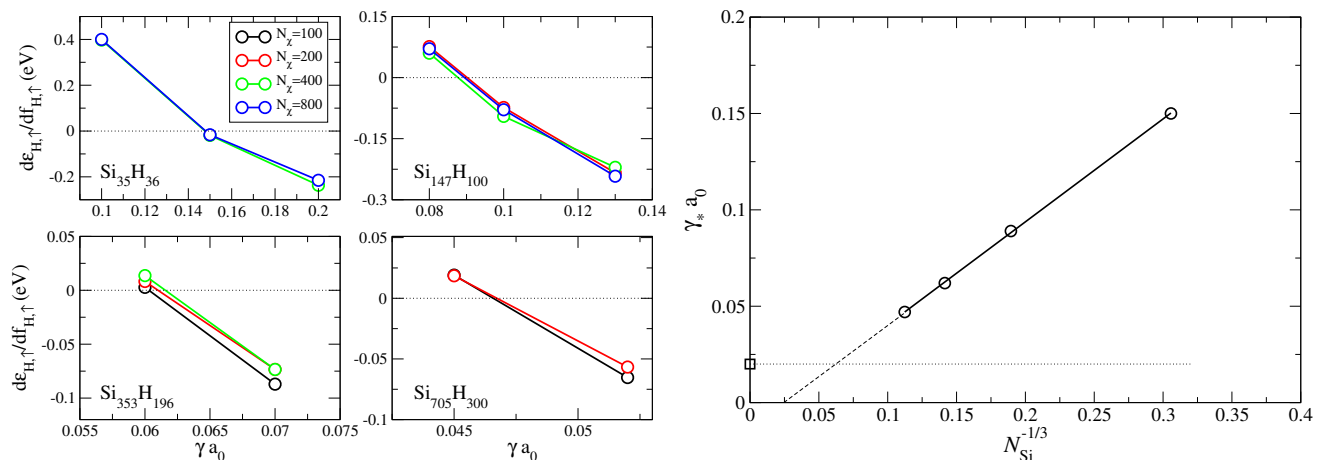


Figure 1. Left panels: The curvature as a function of γ for the HOMO energy, $\partial\varepsilon_{H,\uparrow}/\partial f_{H,\uparrow}$ for different silicon nanocrystals and for different number of stochastic orbitals used to evaluate the non-local exchange. Right panel: The optimal value of γ determined by Eq. (12) for the selected silicon nanocrystals. The results are best-fitted to $-0.013 + 0.53N_{\text{Si}}^{-1/3}$. The square is the reverse engineered value of γ which yields the experimental band gap of bulk silicon Ref. 62.

IV. RESULTS FOR SILICON NANOCRYSTALS

The new method has been implemented using the BNL functional^{34,35} for a series of hydrogen passivated silicon nanocrystals of varying sizes: $\text{Si}_{35}\text{H}_{36}$, $\text{Si}_{87}\text{H}_{76}$, $\text{Si}_{147}\text{H}_{100}$, $\text{Si}_{353}\text{H}_{196}$ and $\text{Si}_{705}\text{H}_{300}$ with real-space grids of 60^3 , 64^3 , 70^3 , 90^3 and 108^3 grid-points, respectively. We solve the generalized KS equations fully self-consistently using the Chebyshev-filtered subspace acceleration^{64,65} to obtain the occupied and low lying unoccupied eigenfunctions and eigenvalues.

The curvature for the different NCs, estimated from a forward difference formula $-\frac{\partial\varepsilon_{H,\uparrow}(c)}{\partial c} \approx \frac{\varepsilon_{H,\uparrow}(0) - \varepsilon_{H,\uparrow}(\delta)}{\delta}$ with $\delta = 0.125$, is plotted as a function of γ in Fig. 1. The curvature is a decreasing function of γ and has a node at the optimal value of the range parameter γ_* . For each NC the curvature results are shown for several values of the number of stochastic orbitals N_χ . We find that the statistical fluctuations near γ_* become smaller as the system grows and can be reduced with proper choice of N_χ . For example, for the larger system the results near γ_* can be converged with only $N_\chi \approx 200$ compared to the total number of occupied states for this system which is 1560. The reduction of these fluctuations is partially due to the decrease of γ_* itself as the NC size increases (this decrease is shown in the right panel of Fig. 1), leading to a smaller contribution of the non-local exchange to the orbital energies.

The results in the right panel of the figure also show that γ_* closely follows a linear function of $N_{\text{Si}}^{-1/3}$. We expect that for larger NCs with $N_{\text{Si}} > 2500$, this linear relation will break down and the optimal range parameter will converge to the bulk value, which through reverse engineering⁶² can be estimated as $\gamma_*^\infty = 0.02a_0^{-1}$ (shown as a horizontal dotted line). Such a localization-induced by the exchange has been seen for 1D conjugated polymers⁶⁶ but not for bulk solids like silicon, likely due to the enormity of the calculation.

In Fig. 2 we plot the highest occupied molecular orbital (HOMO, left panel) and lowest unoccupied molecular orbital (LUMO, right panel) energies obtained from the relations⁶¹

$$\begin{aligned} \varepsilon_{H,\uparrow} &= - \left. \frac{\partial E_{\text{RSH}}^\gamma [\rho_\uparrow, \rho_\downarrow]}{\partial c} \right|_{c \rightarrow 0^+} \\ \varepsilon_{L,\uparrow} &= - \left. \frac{\partial E_{\text{RSH}}^\gamma [\rho_\uparrow, \rho_\downarrow]}{\partial c} \right|_{c \rightarrow 0^-} \end{aligned} \quad (22)$$

respectively, as a function of N_χ at γ_* . We find that determining the HOMO and LUMO energies using the above first derivative relations reduces the noise compared to obtaining their values directly from the eigenvalues. Clearly $\varepsilon_{H,\uparrow}$ and $\varepsilon_{L,\uparrow}$ converge as N_χ increases. Moreover, as the system size increases the fluctuations in $\varepsilon_{H,\uparrow}$ and $\varepsilon_{L,\uparrow}$ decrease for a given value of N_χ , consistent with the discussion above. This is evident from the plot of the differences between the frontier orbital energies at adjacent values of N_χ .

In the lower panel of Fig. 3 we plot the converged (with respect to N_χ) HOMO and LUMO energies at γ_* for the series of silicon NCs. For the smallest system ($\text{Si}_{35}\text{H}_{36}$) we compare the stochastic approach developed here with a deterministic RSH calculation using a non-local exchange with all occupied orbitals and obtaining the Coulomb convolution integrals with FFTs, thereby eliminating any source of statistical error. The purpose is to show that when the stochastic results are converged the agreement with a deterministic calculation is perfect on a relevant magnitude of energy. We find that the HOMO energy increases and the LUMO energy decreases with the size of the NC. This is consistent with our recent calculations on silicon NCs using the stochastic GW approach, albeit the fact that there is a small shift in the quasi-particle energies obtained from the stochastic RSH approach compared to the *s*GW. Indeed, a similar shift has been reported previously for much smaller silicon NCs.⁴⁰ However, the source

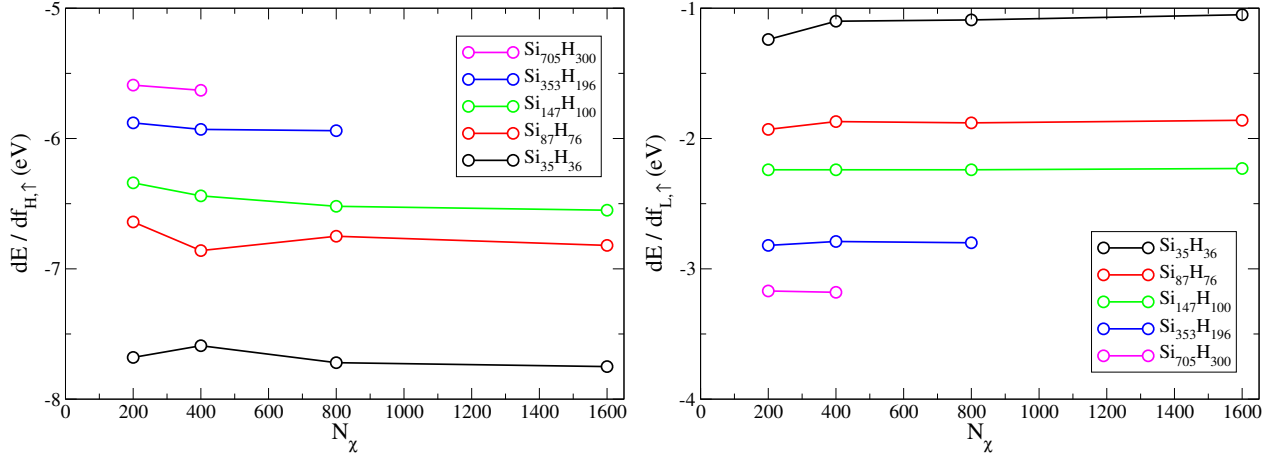


Figure 2. Convergence of the HOMO (H) energy (left panel) and the LUMO ($L = H + 1$) energy (right panel) with number of stochastic orbitals N_χ for silicon nanocrystals using the BNL range-separated functional.

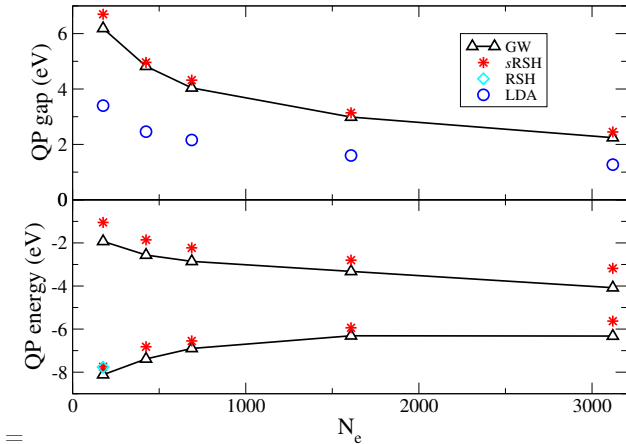


Figure 3. Lower panel: Comparison of the HOMO and LUMO energies obtained using the s GW approach (black triangles) and the stochastic RSH within the BNL functional (red asterisk) for a series of silicon nanocrystals. The cyan diamond represent the deterministic RSH within the BNL functional. Upper panel: The corresponding quasiparticle band gaps. Also shown is the DFT result within the LDA (blue circles).

of this discrepancy is not clear, particularly, since the GW calculations were done within the so called G_0W_0 limit, and the OT-RSH often provides better quasiparticle energies in comparison to experiments.⁴¹ In the upper panel of Fig. 3 we plot the fundamental (quasiparticle) gaps. Here, the agreement with the s GW approach is rather remarkable, especially compared to the LDA results which significantly underestimate the quasiparticle gap across all sizes studied.

In Table I we provide numerical details of the calculations for the smallest and largest NC studied. We report the results for the HOMO and LUMO orbital energies for two different choices of N_χ . Comparing these two values we can conclude that the statistical errors for the LUMO are very small (≈ 0.01 eV) for the largest NC and even the HOMO has small errors of around ≈ 0.05 eV. Moreover,

similar or even larger statistical errors are observed for the smaller NC for much larger values of N_χ , indicating that for a given accuracy the number of stochastic orbitals decreases with the system size. This is partially correlated with the reduction of γ_* with the system size, as discussed above.

V. SUMMARY

We have developed a stochastic representation for the non-local exchange operator in order to combine real-space/plane-waves methods with optimally-tuned range-separated hybrid functionals within the generalized Kohn-Sham scheme. Our formalism uses two principles, one is a stochastic decomposition the Coulomb convolution integrals and the other is the representation of the density matrix using stochastic orbitals. Combining these two ideas leads to a significant reduction of the computational effort and, for the systems studied in this work, to a reduction of the computational scaling of the non-local exchange op-

System	Functional	N_χ	ε_H (eV)	ε_L (eV)	ε_g (eV)	$T_{CPU}^{(c)}$
$Si_{35}H_{36}$	LDA	-	-6.13	-2.73	3.40	1.6
	BNL ^(a)	800	-7.72	-1.09	6.63	16
		1600	-7.75	-1.05	6.70	30
$Si_{705}H_{300}$	LDA	-	-5.13	-3.85	1.28	132
	BNL ^(b)	200	-5.59	-3.18	2.41	234
		400	-5.63	-3.17	2.46	310

(a) $\gamma_* = 0.148 a_0^{-1}$

(b) $\gamma_* = 0.047 a_0^{-1}$

(c) In CPU-hrs

Table I. Optimally-tuned BNL frontier orbital energies and computational times T_{CPU} vs. number of stochastic orbitals N_χ for two (medium and large) silicon clusters. Values for LDA are also given for comparison. As the system size grows, T_{CPU} for the optimally-tuned BNL decreases relative to the LDA timings due to decrease of γ_* .

erator, at the price of introducing a statistical error. The statistical error is controlled by increasing the number of stochastic orbitals and is also found to reduce with the system size. Applications to silicon NCs of varying sizes show relatively good agreement for the band-edge quasiparticle excitations in comparison to a many-body perturbation approach within the *s*GW approximation and excellent agreement for the fundamental band gap. The stochastic approach has a major advantage over the *s*GW by providing a self-consistent Hamiltonian which is central for post-processing, for example in conjunction with a real-time Bethe–Salpeter approach.⁵⁵ The results shown here for $N_e > 3000$ and $N_g > 10^6$ are the largest reported so far for the optimally-tuned range-separated generalized Kohn–Sham approach.

ACKNOWLEDGMENTS

R. B. and E. R. gratefully thank the Israel Science Foundation–FIRST Program (Grant No. 1700/14). R.B. gratefully acknowledges support for his sabbatical visit by the Pitzer Center and the Kavli Institute of the University of California, Berkeley. D. N. and E. R. acknowledge support by the NSF, grants CHE-1112500 and CHE-1465064, respectively.

Appendix A: treatment of the $k = 0$ term

For accelerating convergence, it turns out to be better to remove the $\tilde{u}_C^\gamma(\mathbf{k} = \mathbf{0})$ term from the the random vector expression representing the interaction, i.e.,

$$\zeta(\mathbf{r}) = (2\pi)^{-3} d\mathbf{k} \sum_{\mathbf{k} \neq \mathbf{0}} \sqrt{\tilde{u}_C^\gamma(\mathbf{k})} e^{i\varphi(\mathbf{k})} e^{i\mathbf{k}\cdot\mathbf{r}}.$$

This is because in practice the $\tilde{u}_C^\gamma(\mathbf{k} = \mathbf{0})$ term is very large. Analytically, this term is easily shown to commute with the Fock Hamiltonian and simply contribute a constant (times the occupation) to the eigenvalues and to the total energy, so it can be added a-posteriori:

$$\hat{k}_\sigma^\gamma \phi_{j,\sigma}(\mathbf{r}) \rightarrow \hat{k}_\sigma^\gamma \phi_{j,\sigma}(\mathbf{r}) - f_{j,\sigma} v_{0X},$$

$$\varepsilon_{j,\sigma}^\gamma \rightarrow \varepsilon_{j,\sigma}^\gamma - f_{j,\sigma} v_{0X},$$

$$K[\rho_\uparrow, \rho_\downarrow] \rightarrow K[\rho_\uparrow, \rho_\downarrow] - \frac{1}{2} v_{0X} \sum f_{j\sigma}^2,$$

where

$$v_{0X} \equiv (2\pi)^{-3} d\mathbf{k} \tilde{u}_C^\gamma(\mathbf{k} = \mathbf{0}).$$

* dxn@chem.ucla.edu

† eran.rabani@berkeley.edu

‡ roi.baer@huji.ac.il

¹ W. Kohn and L. J. Sham, Phys. Rev. **140**, A1133 (1965).

² S. Ogut, J. R. Chelikowsky, and S. G. Louie, Phys. Rev. Lett. **83**, 1270 (1999).

³ R. W. Godby and I. D. White, Phys. Rev. Lett. **80**, 3161 (1998).

⁴ A. M. Teale, F. De Proft, and D. J. Tozer, J. Chem. Phys. **129**, 044110 (2008).

⁵ C.-O. Almbladh and U. von Barth, Phys. Rev. B **31**, 3231 (1985).

⁶ J. P. Perdew, R. G. Parr, M. Levy, and J. L. Balduz, Phys. Rev. Lett. **49**, 1691 (1982).

⁷ L. J. Sham and M. Schlüter, Phys. Rev. Lett. **51**, 1888 (1983).

⁸ L. Hedin, Phys. Rev. **139**, A796 (1965).

⁹ M. S. Hybertsen and S. G. Louie, Phys. Rev. Lett. **55**, 1418 (1985).

¹⁰ R. Del Sole, L. Reining, and R. Godby, Phys. Rev. B **49**, 8024 (1994).

¹¹ L. Steinbeck, A. Rubio, L. Reining, M. Torrent, I. White, and R. Godby, Comput. Phys. Commun. **125**, 05 (1999).

¹² A. Fleszar, Phys. Rev. B **64** (2001).

¹³ G. Onida, L. Reining, and A. Rubio, Rev. Mod. Phys. **74**, 601 (2002).

¹⁴ P. Rinke, A. Qteish, J. Neugebauer, C. Freysoldt, and M. Scheffler, New J. Phys. **7**, (2005).

¹⁵ C. Friedrich and A. Schindlmayr, NIC Series **31**, 335 (2006).

¹⁶ M. Shishkin and G. Kresse, Phys. Rev. B **75**, 235102 (2007).

¹⁷ P. E. Trevisanutto, C. Giorgetti, L. Reining, M. Ladisa, and V. Olevano, Phys. Rev. Lett. **101**, 226405 (2008).

¹⁸ C. Rostgaard, K. W. Jacobsen, and K. S. Thygesen, Phys. Rev. B **81**, 085103 (2010).

¹⁹ P. Liao and E. A. Carter, Phys. Chem. Chem. Phys. **13**, 15189 (2011).

²⁰ X. Blase, C. Attaccalite, and V. Olevano, Phys. Rev. B **83**, 115103 (2011).

²¹ I. Tamblyn, P. Darancet, S. Y. Quek, S. A. Bonev, and J. B. Neaton, Phys. Rev. B **84**, 201402 (2011).

²² G. Samsonidze, M. Jain, J. Deslippe, M. L. Cohen, and S. G. Louie, Phys. Rev. Lett. **107**, 186404 (2011).

²³ N. Marom, F. Caruso, X. Ren, O. T. Hofmann, T. Körzdörfer, J. R. Chelikowsky, A. Rubio, M. Scheffler, and P. Rinke, Phys. Rev. B **86**, 245127 (2012).

²⁴ M. van Setten, F. Weigend, and F. Evers, J. Chem. Theory Comput. **9**, 232 (2012).

²⁵ T. A. Pham, H.-V. Nguyen, D. Rocca, and G. Galli, Phys. Rev. B **87**, 155148 (2013).

²⁶ A. Seidl, A. Görling, P. Vogl, J. A. Majewski, and M. Levy, Phys. Rev. B **53**, 3764 (1996).

²⁷ J. Heyd, J. E. Peralta, G. E. Scuseria, and R. L. Martin, J. Chem. Phys. **123**, 174101 (2005).

²⁸ I. C. Gerber, J. G. Angyan, M. Marsman, and G. Kresse, J. Chem. Phys. **127**, 054101 (2007).

²⁹ E. N. Brothers, A. F. Izmaylov, J. O. Normand, V. Barone, and G. E. Scuseria, J. Chem. Phys. **129**, 011102 (2008).

³⁰ V. Barone, O. Hod, J. E. Peralta, and G. E. Scuseria, Acc. Chem. Res. **44**, 269 (2011).

- ³¹ A. Savin and H. J. Flad, *Int. J. Quantum Chem.* **56**, 327 (1995).
- ³² H. Iikura, T. Tsuneda, T. Yanai, and K. Hirao, *J. Chem. Phys.* **115**, 3540 (2001).
- ³³ T. Yanai, D. P. Tew, and N. C. Handy, *Chem. Phys. Lett.* **393**, 51 (2004).
- ³⁴ R. Baer and D. Neuhauser, *Phys. Rev. Lett.* **94**, 043002 (2005).
- ³⁵ E. Livshits and R. Baer, *Phys. Chem. Chem. Phys.* **9**, 2932 (2007).
- ³⁶ O. A. Vydrov and G. E. Scuseria, *J. Chem. Phys.* **125**, 234109 (2006).
- ³⁷ J. D. Chai and M. Head-Gordon, *Phys. Chem. Chem. Phys.* **10**, 6615 (2008).
- ³⁸ E. Livshits and R. Baer, *J. Phys. Chem. A* **112**, 12789 (2008).
- ³⁹ R. Baer, E. Livshits, and U. Salzner, *Annu. Rev. Phys. Chem.* **61**, 85 (2010).
- ⁴⁰ T. Stein, H. Eisenberg, L. Kronik, and R. Baer, *Phys. Rev. Lett.* **105**, 266802 (2010).
- ⁴¹ L. Kronik, T. Stein, S. Refaely-Abramson, and R. Baer, *J. Chem. Theory Comput.* **8**, 1515 (2012).
- ⁴² T. Körzdörfer, R. M. Parrish, N. Marom, J. S. Sears, C. D. Sherrill, and J.-L. Brédas, *Phys. Rev. B* **86**, 205110 (2012).
- ⁴³ D. Jacquemin, B. Moore, A. Planchat, C. Adamo, and J. Autschbach, *J. Chem. Theory Comput.* **10**, 1677 (2014).
- ⁴⁴ T. Stein, J. Autschbach, N. Govind, L. Kronik, and R. Baer, *J. Phys. Chem. Lett.* **3**, 3740 (2012).
- ⁴⁵ D. Neuhauser, Y. Gao, C. Arntsen, C. Karshenas, E. Rabani, and R. Baer, *Phys. Rev. Lett.* **113**, 076402 (2014).
- ⁴⁶ R. Baer, D. Neuhauser, and E. Rabani, *Phys. Rev. Lett.* **111**, 106402 (2013).
- ⁴⁷ D. Neuhauser, R. Baer, and E. Rabani, *J. Chem. Phys.* **141**, 041102 (2014).
- ⁴⁸ R. Baer and E. Rabani, *Nano Lett.* **12**, 2123 (2012).
- ⁴⁹ D. Neuhauser, E. Rabani, and R. Baer, *J. Chem. Theory Comput.* **9**, 24 (2013).
- ⁵⁰ D. Neuhauser, E. Rabani, and R. Baer, *J. Phys. Chem. Lett.* **4**, 1172 (2013).
- ⁵¹ Q. Ge, Y. Gao, R. Baer, E. Rabani, and D. Neuhauser, *J. Phys. Chem. Lett.* **5**, 185 (2013).
- ⁵² Y. Gao, D. Neuhauser, R. Baer, and E. Rabani, *J. Chem. Phys.* **142**, 034106 (2015).
- ⁵³ R. Baer and D. Neuhauser, *J. Chem. Phys.* **137**, 051103 (2012).
- ⁵⁴ Y. Cytter, D. Neuhauser, and R. Baer, *J. Chem. Theory Comput.* **10**, 4317 (2014).
- ⁵⁵ E. Rabani, R. Baer, and D. Neuhauser, *Phys. Rev. B* **91**, 235302 (2015).
- ⁵⁶ R. Kosloff, *J. Phys. Chem.* **92**, 2087 (1988).
- ⁵⁷ R. Kosloff, *Annu. Rev. Phys. Chem.* **45**, 145 (1994).
- ⁵⁸ A. Savin, *Beyond the Kohn-Sham Determinant* (World Scientific, Singapore, 1995), p. 129.
- ⁵⁹ R. M. Dreizler and E. K. U. Gross, *Density Functional Theory: An Approach to the Quantum Many Body Problem* (Springer, Berlin, 1990).
- ⁶⁰ T. Stein, L. Kronik, and R. Baer, *J. Am. Chem. Soc.* **131**, 2818 (2009).
- ⁶¹ J. Janak, *Phys. Rev. B* **18**, 7165 (1978).
- ⁶² H. R. Eisenberg and R. Baer, *Phys. Chem. Chem. Phys.* **11**, 4674 (2009).
- ⁶³ D. Kosloff and R. Kosloff, *J. Comput. Phys.* **52**, 35 (1983).
- ⁶⁴ Y. Zhou, Y. Saad, M. L. Tiago, and J. R. Chelikowsky, *Phys. Rev E* **74**, 066704 (2006).
- ⁶⁵ K. Khoo, M. Kim, G. Schofield, and J. R. Chelikowsky, *Phys. Rev. B* **82**, 064201 (2010).
- ⁶⁶ V. Vlček, H. R. Eisenberg, G. Steinle-Neumann, and R. Baer, arXiv preprint arXiv:1509.05222 (2015).